

Article

The Influence of the Reaction Parameters on the Synthesis of Fatty Acid Octyl Esters and Investigation of Applications Properties of Its Blends with Mineral Diesel

Mia Gotovuša ¹, Marko Racar ¹ , Lucija Konjević ², Jelena Parlov Vuković ³ and Fabio Faraguna ^{1,*} 

¹ Faculty of Chemical Engineering and Technology, University of Zagreb, Marulićev Trg 19, 10000 Zagreb, Croatia

² Adriatic Biodiesel d.o.o, Netretić 31, 47271 Netretić, Croatia

³ Ruđer Bošković Institute, Bijenička Cesta 54, 10000 Zagreb, Croatia

* Correspondence: fabio.faraguna@fkit.hr

Abstract: The first aim of this paper is to study the influence of four parameters of the transesterification reaction—reaction temperature (40–80 °C), time (1–3 h), the molar ratio of 1-octanol to sunflower oil (4:1–10:1) and mass fraction of the catalyst (1–3 wt%)—on the conversion of oil to biodiesel (octyl esters of fatty acids), with potassium hydroxide as a catalyst. The highest conversion, of 99.2%, was obtained at 60 °C, a molar ratio of 1-octanol to sunflower oil of 10:1, and with 2 wt% of the catalyst after an hour. The optimal conditions determined with response surface methodology (RSM) when aiming for the lowest possible parameter values and a conversion of 95% or higher were a temperature of 40 °C, time of 1 h, 1-octanol to oil molar ratio at 8.11:1 and mass fraction of catalyst of 2.01%. Furthermore, post-synthesis and purification (>99%), the application properties of pure fatty acid octyl esters (FAOCE) and their blends with mineral diesel and 1-octanol were evaluated. Standardized tests were conducted to measure the fuel's density, viscosity, cold filter plugging point (CFPP), and lubricity. The addition of FAOCE in mineral diesel increases its density, viscosity, and lubricity. When added up to 20 vol%, FAOCE did not have an influence on the blend's CFPP value. Still, all the blend property values fell within the limits required by standard EN 590.

Keywords: biodiesel; transesterification; 1-octanol; fatty acid octyl esters; blends with mineral diesel



Citation: Gotovuša, M.; Racar, M.; Konjević, L.; Parlov Vuković, J.; Faraguna, F. The Influence of the Reaction Parameters on the Synthesis of Fatty Acid Octyl Esters and Investigation of Applications Properties of Its Blends with Mineral Diesel. *Energies* **2023**, *16*, 3071. <https://doi.org/10.3390/en16073071>

Academic Editors: João Fernando Pereira Gomes and Toufik Boushaki

Received: 26 February 2023

Revised: 19 March 2023

Accepted: 26 March 2023

Published: 28 March 2023



Copyright: © 2023 by the authors. Licensee MDPI, Basel, Switzerland. This article is an open access article distributed under the terms and conditions of the Creative Commons Attribution (CC BY) license (<https://creativecommons.org/licenses/by/4.0/>).

1. Introduction

Over the past couple of decades, the environmental consequences of the intense continuous use of fossil fuels in the energy sector have come to the forefront. Increased greenhouse gas emissions have caused climate changes, i.e., rise in global temperatures, melting of the polar ice caps, and rise in the sea level, just to name a few. As a result, researchers focused on finding alternative ways to cater to the rising energy demands and mend the current environmental issues by developing renewable, biodegradable, and sustainable biofuels.

Biodiesel as a renewable fuel can be used in diesel engines, both alone and as a part of binary blends with mineral diesel [1,2]. Due to its similar properties, it requires little to no improvement to be used in the engines [3]. Increasing environmental concerns have led to the rise in the use of alternative fuels and their production is being studied more and more, from the use of various natural material sources [4], to observing the properties of the pure and blended final products [5], to producing them through different catalytical routes [6]. Biodiesel, as an alternative fuel obtained by transesterification, consists of long-chain fatty acid alkyl esters (FAAE).

These alternative fuels are derived from renewable feedstock, such as vegetable oils (rapeseed, sunflower, soybeans, coconut, jatropha, palm, used cooking oil) [7], bioalcohols (bioethanol, biobutanol) [7] or waste animal fats (chicken fat, beef tallow, pork lard, poultry

fats) [8]. Depending on the prevalence of alcohol use, the most common biodiesels are fatty acid methyl esters (FAME) and fatty acid ethyl esters (FAEE), yielded from methanol and ethanol [9].

In the literature, higher alcohols have been used for biodiesel syntheses such as 1-propanol [10], 2-propanol [11], 1-butanol [12,13], 2-butanol [14], isobutanol [15], 1-pentanol [16], isopentanol [17], 1-hexanol [18], 1-heptanol [18], 1-octanol [18], 1-decanol [18], 1-dodecanol [18], and benzyl alcohol [18], but not studied in detail. Moreover, the use of higher alcohols in alcohol/diesel blends can significantly improve their properties [19]. This refers in particular to the engine performance, as well as its emission and combustion characteristics. Some of the main reasons for the more common application of higher alcohols over methanol or ethanol include their higher calorific value, higher flash point and lower vapor pressure [20], higher cetane number [21], higher flame speed [22], better miscibility [23], improvement of kinematic viscosities [24], as well as a noticeable decrease in corrosion [25]. The alcohol 1-octanol is usually produced by iterative oligomerization via the Ziegler process [26]. On the other hand, renewable feedstocks, such as common vegetable oils and animal fats, do not contain octanoic acid leading the research to alternative ways of production from renewable feedstock. These processes are the reversal of β -oxidation [27], extended 1-butanol pathway [28], rerouting the branch-chain amino acid biosynthesis [29], and other pathways that include different engineered microorganisms, for example, engineered cyanobacteria [30] or bacteria *Escherichia coli* [31]. However, 1-octanol, as a medium-chain alcohol, is toxic to microbes because it has a negative effect on the cell membrane and enzyme selectivity [32], keeping these pathways in the proof-of-concept stage [33]. There are some studies in the literature that investigated the application of 1-octanol in biodiesel synthesis, where this alcohol reacted with a different feedstock [34]. The research showed how the presence of 1-octanol in binary blends with the obtained biodiesel (*Calophyllum Inophyllum* methyl ester) influences compression ignition engine characteristics. It was found that the calorific value of the blends decreased due to their oxygen content. In addition, the ignition delay was prolonged while the peaks of in-cylinder pressure and heat release rates generated during the premixed mode of combustion were higher. Blends with higher content of 1-octanol also have lower carbon monoxide and smoke emissions.

Previous studies described various ways of synthesizing fatty acid octyl esters. Triglycerides were converted to fatty acid octyl esters by one-step acid-catalyzed heterogeneous transesterification [35]; two-step processes with two transesterifications by homogeneous base catalysis [36], biocatalysis followed by acid-catalyzed esterification [37], two-step biocatalysis [38] and separation of free fatty acids and subsequent acid-catalyzed esterification [39]; and three-step processes where triglycerides were saponified, converted to free fatty acids and then esterified with N-doped graphene oxide [40]. Few studies focused just on the esterification by biocatalysis [41–43] and photocatalysis [44,45] of free fatty acids, i.e., the product of the first step. All of the mentioned studies, except the studies with heterogeneous acid-catalyzed transesterification [35], had two- or three-step processes that included esterification or direct esterification from free fatty acids. On the other hand, sunflower oil was used to perform two acid-catalyzed transesterifications by firstly synthesizing FAEE and then performing transesterification of FAEE with 1-octanol to obtain FAOCE [36]. The multi-step methodologies have many disadvantages. In general, the increase in steps leads to additional costs and lower yield due to the need to obtain free fatty acids from vegetable oils which can result in incomplete conversions and losses during the purification steps. On the other hand, the synthesis requires two transesterifications, two separate purification steps, and more chemicals (more catalyst for the two-step process, additional ethanol), which in turn generates more waste. The transesterification of triglycerides (sunflower and rubber seed oil) was also studied with a heterogeneous acid catalyst in a continuous flow process [35]. The transesterification required a high 1-octanol to oil molar ratio (15:1) and high temperature (170 °C), reaching conversions up to 90.2%. That is why, this work aims to achieve high yields at milder reaction conditions and to describe the influence of process

parameters (temperature, time, molar ratio of the reactants, and mass fraction of catalyst) on the transesterification of sunflower oil and 1-octanol in one step via homogeneous base catalysis with KOH as an economical and widely available catalyst. The production of biodiesel from 1-octanol via transesterification using base catalysis has not been investigated comprehensively and the results of this study show that high conversions can be achieved with long-chain alcohols using the investigated parameters. The results may be useful for the meta-analysis and comparison of the influence of parameters with similar research that used different alcohols or triglycerides. The concept of biodiesel production from higher alcohols is attractive because the removal of residual alcohol, such as 1-octanol, after transesterification is not so critical [46]. The complete removal of 1-octanol is not necessary; hence, the costs of biodiesel purification could be reduced.

The density of biodiesel is an important physical property, required for the overall process equipment design because it mainly affects the fuel's equivalence ratio distribution, as well as its spray momentum [47]. Viscosity represents the flow resistance of the fuel [48]. For example, biodiesel made from sunflower oil can reach values up to 1.55 times higher than those, of mineral diesel [49]. Fuel injection, followed by spray formation through atomization is the main process that depends on the fuel's viscosity. The higher the viscosity, the lower the spray cone angle, and the higher the spray penetration and droplet size [50]. In terms of the chemical structures, the long saturated straight chain moieties, either of fatty acids, alcohols, or both, may increase biodiesel's kinematic viscosity [51].

Numerous studies that investigated the effect of blending a particular biodiesel with mineral diesel on the blend lubricity, i.e., palm oil biodiesel [52], Jatropha biodiesel [53], or rapeseed biodiesel [54], found that increasing the biodiesel content resulted in a reduction of friction and wear of the engine sliding parts. Biodiesel itself is characterized by its poor low-temperature properties, i.e., cloud point (CP), cold filter plugging point (CFPP) and pour point (PP). Crystallization occurs at a temperature of CP, fuel begins to plug the engine filter at CFPP, whereas, at PP, fuel does not pour anymore [55]. The reason for these properties can be found in the fatty acid composition. Higher CFPP values belong to highly saturated fatty acids due to the increase in fatty acids' melting points with their saturation [56]. Therefore, biodiesel's low-temperature properties can be modified by blending, e.g., mineral diesel in different volume ratios [57].

The first objective of this study was to conduct the experiments according to the design of experiments (DoE) (Box–Behnken design), and to determine, as well as experimentally validate, the optimal conditions using response surface methodology (RSM). The second objective was to purify and blend the synthesized fuel with mineral diesel alone or with 1-octanol as the third component to determine how the application properties (i.e., density, viscosity, cold filter plugging point, and lubricity) would change by increasing the volume fraction of biodiesel added. In addition, the pure components and their blends were measured using a goniometer and differential scanning calorimetry, to obtain surface tension and crystallization values, respectively. The novelty of this study lies within the systematic approach to the synthesis, reaction optimization, and application property analysis of biodiesel obtained from non-conventional, higher alcohol 1-octanol, and their blends with commercial mineral diesel. Considering the potential to improve fuel properties, which different biodiesels have shown based on the literature, our aim was to investigate how fatty acid octyl esters interact with fossil fuel and could their use possibly eliminate the need for additional additives.

2. Materials and Methods

Materials for the reaction of transesterification were 1-octanol (98%, BHB Prolabo), and sunflower oil (Zvijezda plus d.o.o., molar mass of 876.45 g/mol), and they were used as received. Potassium hydroxide (89.5%, Sigma-Aldrich, St. Louis, MO, USA) was used as the catalyst and was previously vacuum dried for 30 min at 100 °C. For purification purposes, ortho-phosphoric acid (85.6%, Lach:NER) was used. The diesel used in this study for the preparation of binary and ternary blends was without additives and consisted of 80% of

aliphatic and 20% of aromatic hydrocarbons. It had low amount of sulfur (7.0 mg/kg), density of 826.3 kg/m³, and cold filter plugging point of −8 °C.

Box–Behnken statistical plan was used for the design of experiments (DoE) that consisted of 29 experiments. The DoE was based on four parameters at three levels with three central points. The levels of the parameters (temperature, time, molar ratio of reactants, mass fraction of catalyst) are given in Table 1.

Table 1. The levels of parameters for biodiesel production.

Variable/Range	−1	0	+1
Temperature (°C)	40	60	80
Time (h)	1.00	2.00	3.00
A/O molar ratio (mol/mol)	4.00	7.00	10.00
Catalyst concentration (wt%)	1.00	2.00	3.00

Biodiesel synthesis was conducted in glass tubes submerged into an oil bath and mixed with a magnetic stirrer. The reactants (sunflower oil and 1-octanol) and catalyst (potassium hydroxide) were weighed separately, with the desired mass of catalyst dissolved in 1-octanol in one tube and the mass of sunflower oil in the other. All weighted tubes were placed into the oil bath and heated until the set temperature was reached. Immediately after reaching the set temperature, the contents were mixed. The transesterification reaction was terminated by dipping the reaction tube into an ice bath. Immediately afterward, a 2 mL sample was taken and frozen for ¹H nuclear magnetic resonance (NMR) analysis. ¹H NMR analysis was performed on Bruker Avance NEO with a frequency of 300 MHz using a C/H dual 5 mm probe. The samples were dissolved in deuterated chloroform. The spectra were obtained with a 5882 Hz spectral width, 10 s delay and 32 scans at a temperature of 298 K. Chemical shifts were referenced to the signal of tetramethylsilane. The conversion of the transesterification reaction was calculated from ¹H NMR spectra by integrating the area below characteristic signals (Supplement Figure S1). Chemical shifts were identified based on the positions and coupling constants of the characteristic protons (H_K), as described in Faraguna et al. [18]. The shift of 2.3 ppm belongs to −OCOCH₂ functional group, characteristic of the hydrogen proton in the structure of the fatty acid analog, while the one of 4.0 ppm belongs to −OCH₂ group. The −OCOCH₂ functional group is characteristic of biodiesel as well as the left-over fatty acid analogs from oil, mono- and diglycerides. The −OCH₂ group is specific only to biodiesel, i.e., fatty acid octyl esters. The conversion of the transesterification reaction, described by the chemical formula (Figure 1), for each experiment was calculated using Equation (1).

$$\text{Conversion, \%} = ((\text{surface area under the signal at 4.0 ppm})/(\text{surface area under the signal at 2.3 ppm})) \times 100 \quad (1)$$

For blending purposes, larger amounts of fatty acid octyl esters were synthesized in a 2 L reactor. Then, synthesized biodiesel was purified from the by-product glycerol and the residual catalyst KOH by washing with aqueous orthophosphoric acid solution at a concentration of 0.2–0.3 wt% and centrifugation. The centrifugation lasted for 20 min at 1950 RCF. To achieve a better biodiesel/1-octanol separation in the upper layer from the bottom layer containing glycerol and KOH, these procedures were repeated four times. The remaining 1-octanol was evaporated in the rotary evaporator, under dynamic vacuum, at 140 °C and 110 rpm. To assess FAOCE's purity after this procedure, the sample was analyzed by NMR and gas chromatography according to EN 14105 which both confirmed low amounts of monoglycerides (<0.01 wt%), diglycerides (0.11 wt%) and triglycerides (leftover oil, <0.01 wt%).

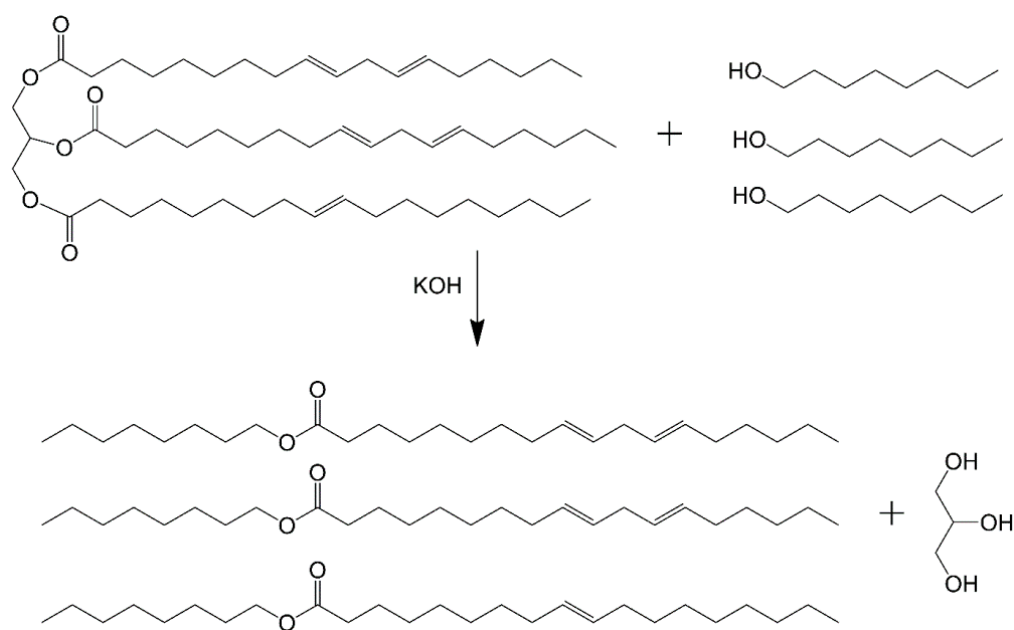


Figure 1. Transesterification of sunflower oil with 1-octanol.

The kinematic viscosity of blends was determined according to ASTM D 7042 using Anton Paar's Stabinger viscometer. The density of blends was determined according to EN ISO 12185 using oscillating U-tube. Cold filter plugging point was measured according to EN 116, while the lubricity results were obtained by measuring the wear scar diameters through high-frequency reciprocating test rig (HFRR), in accordance with the EN ISO 12156-1 standardized test method.

The surface tension of pure components and their blends was determined using DataPhysics OCA 20 Instruments goniometer with software operated CCD camera. Measurements were conducted with a 1.06 mm diameter syringe, via Pendant drop method, through continuous dosing volume of 1.00 μL . For each sample, the measurements were repeated ten times to obtain an average value with a corresponding standard deviation.

Differential scanning calorimetry was conducted using Mettler Toledo's DSC823e. Each sample was weighted to have a mass of 10–15 mg and measured with one cool–heat run with cooling and heating rate of 10 $^{\circ}\text{C}/\text{min}$.

3. Results and Discussion

3.1. Quadratic Model of Transesterification

The influence of each reaction parameter on conversion was determined from the experimental results given in Table 2.

In this equation, *A* represents the temperature ($^{\circ}\text{C}$), *B* the time (hours), *C* the molar ratio of the reactants (mol/mol), and *D* the mass fraction of catalyst (wt%). The obtained model (Equation (2)) consists of coded parameters that are useful for identifying the relative impact of factors by comparing the factor coefficients.

The previously given model (2) describes experimental results well, with the R^2 -value being at 0.97. However, the initial model can be further improved by not including values that showed higher deviation from the rest. Specifically, the result from the first experiment is at the very low end of the conversion range.

Table 2. Calculated conversions of transesterification reaction with corresponding parameter values.

No. of the Experiment	Temperature, T (°C)	Time, t (h)	n (A): n (U), (mol/mol)	Catalyst, w_{cat} . (wt%)	Conversion (%)
1	−1	0	−1	0	31.6 *
2	0	0	−1	1	64.4
3	1	0	0	1	86.7
4	−1	0	0	−1	79.4
5	0	0	0	0	98.44
6	1	0	−1	0	54.7
7	0	0	0	0	94.6
8	0	−1	−1	0	46.3
9	0	1	1	0	98.2
10	0	0	−1	−1	44.8
11	0	0	1	−1	94.8
12	0	−1	0	1	95.6
13	1	1	0	0	95.0
14	0	1	0	−1	88.4
15	−1	1	0	0	88.4
16	1	−1	0	0	94.6
17	1	0	0	−1	84.9
18	0	−1	0	−1	79.4
19	0	1	0	1	96.6
20	0	0	1	1	94.0
21	−1	0	0	1	98.7
22	0	0	0	0	92.2
23	0	0	0	0	86.8
24	0	−1	1	0	99.2
25	−1	0	1	0	98.8
26	−1	−1	0	0	93.7
27	0	1	−1	0	61.9
28	0	0	0	0	93.9
29	1	0	1	0	93.0

*—The first experiment was not included in the making of the second model.

From all the results given in Table 2, an empirical quadratic model was developed:

$$\text{Conversion} = 93.20 + 1.58A + 1.58B + 22.83C + 5.50D + 1.50AB - 7.25AC - 4.50AD - 4.25BC - 2.00BD - 5.00CD - 3.31A^2 + 1.19B^2 - 18.18C^2 - 2.43D^2 \quad (2)$$

The following model was obtained by ignoring the conversion value from the first experiment.

$$\text{Conversion} = 93.20 - 0.0250A + 1.58B + 21.22C + 5.50D + 1.50AB - 2.42AC - 4.50AD - 4.25BC - 2.00BD - 5.00CD - 1.70A^2 + 0.3875B^2 - 16.58C^2 - 3.24D^2 \quad (3)$$

Figure 2 shows the statistical analysis of the model (Equation (3)) and the fitted data.

The obtained results show that the model describes the experimental data well, with all of the experimental data being within the expected limits, meaning the model is significant [58].

Analysis of variance (ANOVA) for the quadratic model (Equation (3)) is given in Table 3.

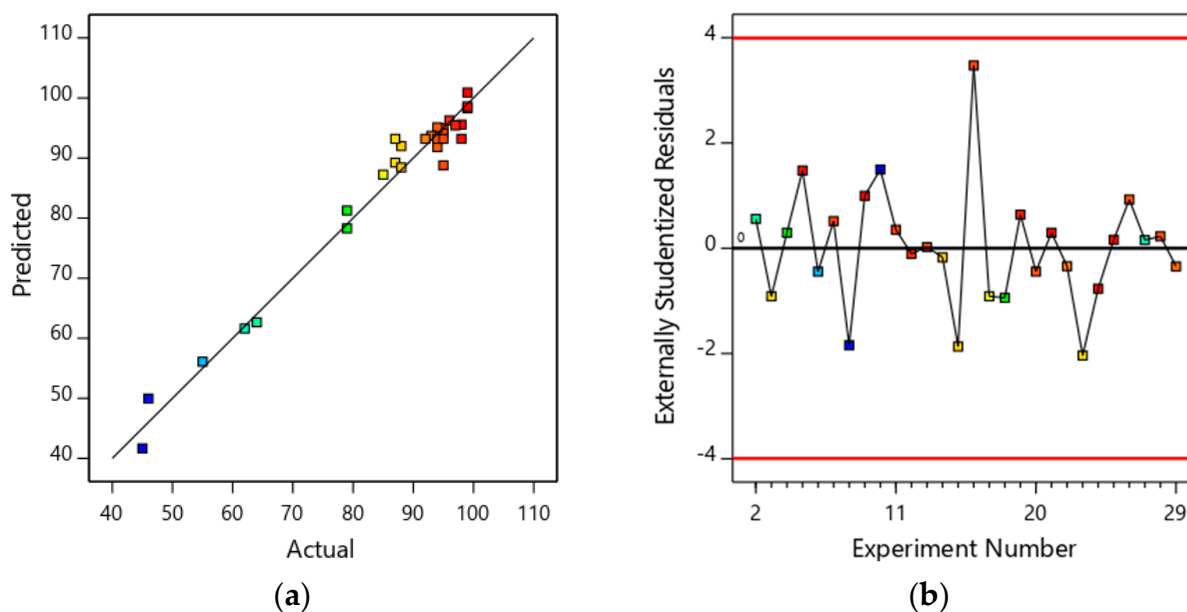


Figure 2. Comparison of predicted and experimentally determined conversion values (a); distribution of residues, r_s depending on the ordinal number of the experiment (b).

Table 3. Part of ANOVA for quadratic model.

Source	Sum of Squares	Degrees of Freedom	Mean Squares	F-Value	Probability p	Source	Sum of Squares
Model	6837.25	14	488.37	33.92	<0.0001		
A	0.0063	1	0.0063	0.0004	0.9837		
B	30.08	1	30.08	2.09	0.1720		
C	4505.01	1	4505.01	312.88	<0.0001		
D	363.00	1	363.00	25.21	0.0002		
AB	9.00	1	9.00	0.6251	0.4434		
AC	14.70	1	14.70	1.02	0.3307		
AD	81.00	1	81.00	5.63	0.0338		
BC	72.25	1	72.25	5.02	0.0432		
BD	16.00	1	16.00	1.11	0.3110		
CD	100.00	1	100.00	6.95	0.0206		
A^2	16.92	1	16.92	1.17	0.2981		
B^2	0.9484	1	0.9484	0.0659	0.8015		
C^2	1608.18	1	1608.18	111.69	<0.0001		
D^2	66.20	1	66.20	4.60	0.0515		
Residual	187.18	13	14.40				
Lack of Fit	120.38	9	13.38	0.8009	0.6425		
Pure Error	66.80	4	16.70				
Cor Total	7024.43	27					

The high F -value of the model of 33.92 implies the model is significant. The R^2 -value equals 0.97. The value of probability p indicates which terms were proven to be of significance to the model ($p < 0.0500$). In this case, the molar ratio of the reactants (C) and the mass fraction of the catalyst (D) are significant model terms and will have the highest influence on the reaction conversion.

3.2. Quadratic Model of Transesterification

Figures 3–5 represent the response surfaces (3D plots) of the obtained model. It can be seen that for a given temperature and time range, when the molar ratio of the reactants is set to a minimum of 4:1, increasing the mass fraction of the catalyst leads to an increase

in the conversion. In addition, the conversion increases gradually within the observed temperature and time range, with that shift being less distinct as the mass fraction of the catalyst increases. The slope of the response surface also changes from a more to a less prominent one when increasing the molar ratio of the reactants from 4:1 to 10:1, while keeping the mass fraction of the catalyst at the minimum value of 1%. The medium value of the molar ratio of the reactants (7:1) also leads to the increase in the reaction conversion with the increase in the mass fraction of the catalyst, but only until the medium value of w_{cat} is reached. Afterward, the slope of the graph surface is reversed, leading to a decrease in reaction conversion with the increase in temperature and reaction time within the investigated limits. However, in this case, this change is not as prominent as with the molar ratio of the reactants reaching its highest value (10:1). Due to the model deficiency in predicting precise results due to the very wide range of the reaction parameters, the predictions around the upper parameters' values are lower than expected and deviate more from experimentally obtained ones.

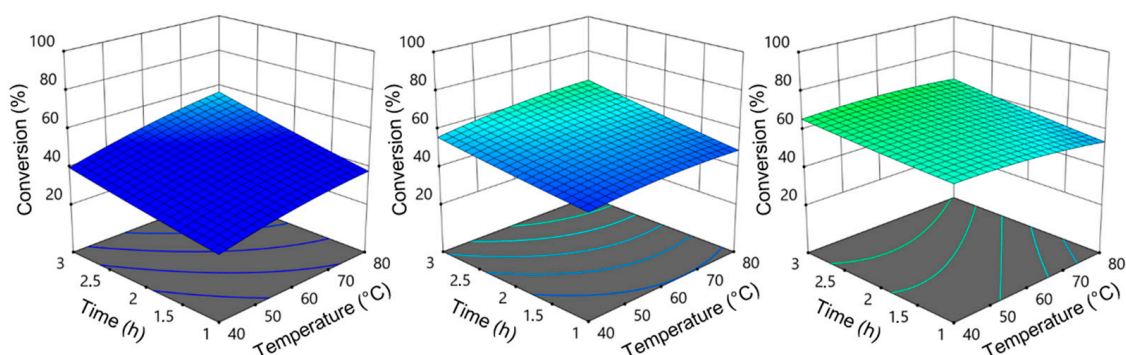


Figure 3. The 3D plots obtained when the molar ratio of the reactants was the lowest (4:1) and the value of the mass fraction of the catalyst was the lowest (1%, (left)), medium (2%, in the (middle)) and the highest (3%, (right)).

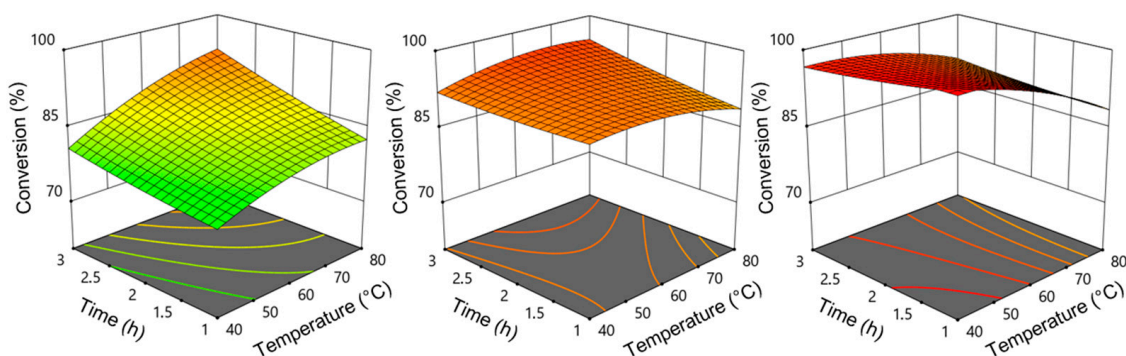


Figure 4. The 3D plots obtained when the molar ratio of the reactants was medium (7:1) and the value of the mass fraction of the catalyst was the lowest (1%, (left)), medium (2%, in the (middle)) and the highest (3%, (right)).

To sum up, when observing the slope of the obtained graphs, it is visible that the higher the molar ratio of the reactants, the smaller the slope of the response surface. This indicates that at the higher molar ratios of the reactants, the increase in the reaction conversion with the rise of reaction temperature and time will be smaller, meaning the reaction is not as sensitive to the change in mentioned parameters. The same decrease in the reaction sensitivity is noted with the increase in catalyst mass fraction with the molar ratio of the reactants being held at a constant value.

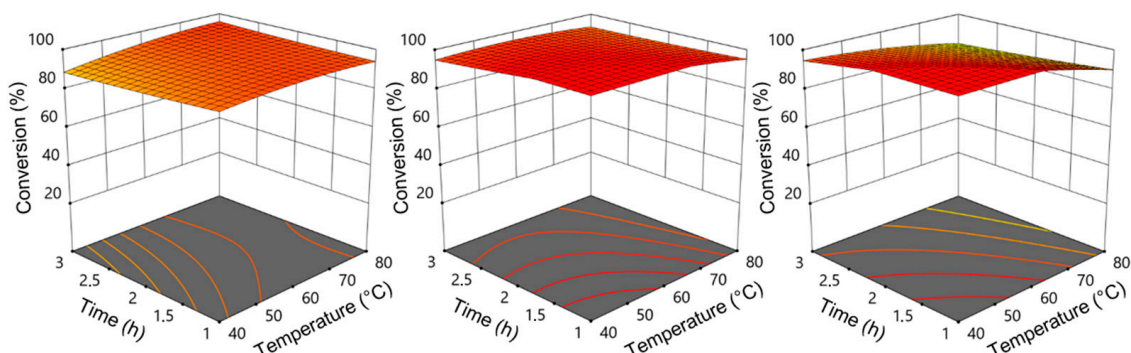


Figure 5. The 3D plots obtained when the molar ratio of the reactants was the highest (10:1) and the value of the mass fraction of the catalyst was the lowest (1%, (**left**)), medium (2%, in the (**middle**)) and the highest (3%, (**right**)).

3.3. Optimization of Biodiesel Production

Numerical optimization of the biodiesel synthesis from sunflower oil and 1-octanol was conducted to find the optimal values of the reaction parameters with the optimization goals given in Table 4.

Table 4. The optimization goals and obtained optimal conditions.

Parameter	Goal	Lower Limit	Upper Limit	Importance	Optimal	Predicted
Temperature (°C)	Min.	40	80	3	40	
Time (h)	Min.	1	3	3	1	
A/O molar ratio (mol/mol)	Min.	4.00	10.00	3	8.11	
Mass fraction of the catalyst (wt%)	Min.	1.00	3.00	3	2.01	
Conversion (%)	In range	95.0	100.0	5		100.0

The optimization goals included the reaction conversion reaching the maximum value (between 95 and 100%), while the reaction temperature, time, molar ratio of the reactants, and mass fraction of the catalyst were set on a minimum value, with a medium significance for each of them. The optimization resulted in following values: $T = 40$ °C, $t = 1$ h, A:O = 8.11 and $w_{\text{cat}} = 2.01$. The reaction conversion predicted for the given set of parameters had a value of 100.0%.

To test the accuracy of this prediction, an additional experiment was conducted at optimal conditions previously given in Table 4. The obtained conversion had a value of 99.0%, confirming the obtained optimal conditions and the model (Equation (3)) accuracy of prediction—the prediction was within the acceptable range of 1%. Compared to the heterogeneous acid catalysis completed by Sreeprasanth et al. [35], base catalysis achieved a nearly complete conversion (99.0% compared to 90.2%) at milder reaction conditions (40 °C compared to 170 °C, and A:O of 8.11:1 compared to 15:1) demonstrating that base catalysis is a more advantageous synthesis route.

3.4. Application Properties of FAOCE and Its Blends with Mineral Diesel and 1-Octanol

FAOCE and its binary blends with non-additivated diesel and ternary blends with non-additivated diesel and 1-octanol were assessed for the application properties as fuels. Table S3 (see Supplement) summarizes the obtained application property results, defined in the EN 590 standard. For comparison purposes, the theoretical values were also calculated by additive equation, as follows for density (e.g.):

$$\rho(\text{mixture}) = \varphi(\text{diesel}) \times \rho(\text{diesel}) + \varphi(\text{FAOCE}) \times \rho(\text{FAOCE}) + \varphi(\text{octanol}) \times \rho(\text{octanol}). \quad (4)$$

The blend application property (density, kinematic viscosity, lubricity, or CFPP) value was calculated as a sum of the product of pure components property values and their volume fraction in the blends.

3.4.1. Kinematic Viscosity of Pure Components and Blends

In order to investigate the influence of FAOCE and 1-octanol on the values of kinematic viscosities of blends, theoretical values were also calculated just to follow the deviations from the measured ones, although this property does not comply with the additive equation. As seen in Figure 6, the kinematic viscosity of biodiesel FAOCE ($4.613 \text{ mm}^2/\text{s}$) is in between the values of mineral diesel ($2.600 \text{ mm}^2/\text{s}$) and 1-octanol ($5.303 \text{ mm}^2/\text{s}$), but closer to the kinematic viscosity of the alcohol. In addition, all the measured and calculated values of the blend viscosities fall within the limits required by the norm EN 590.

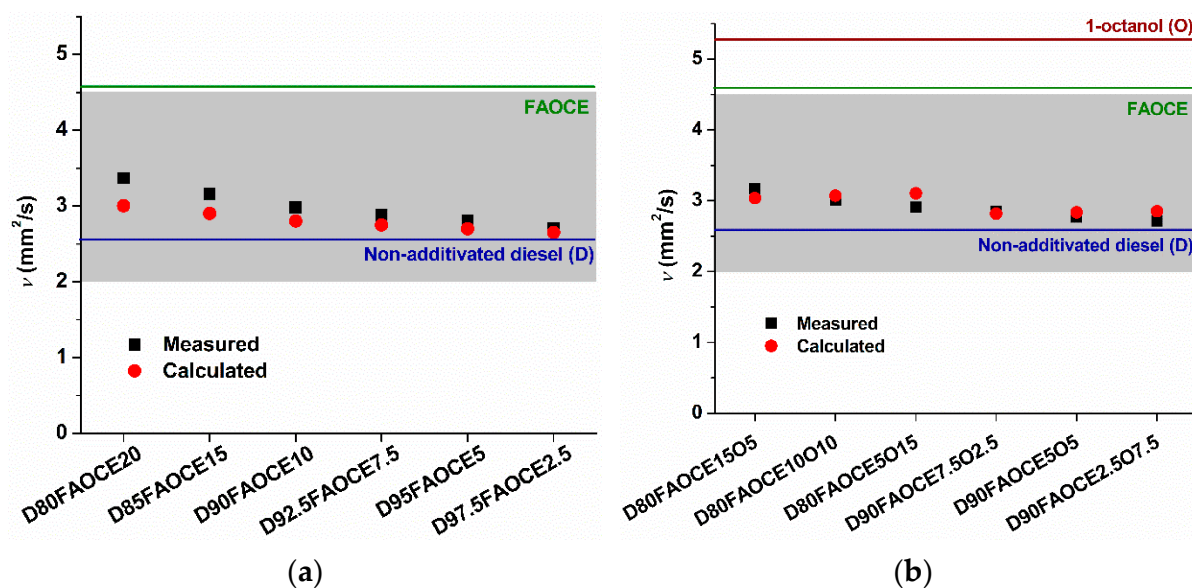


Figure 6. Comparison of measured and calculated kinematic viscosity values of binary (a) and ternary (b) blends of 80, 85, 90, 92.5, 95, and 97.5 vol% diesel.

According to the obtained results, the addition of biodiesel FAOCE to both binary blends with mineral diesel and ternary blends with diesel and 1-octanol increases the blends' viscosity values. This is due to the long nonpolar hydrocarbon chains of fatty acid and alcohol moieties of FAOCE that strongly interact with the aliphatic chains of mineral diesel, increasing the blend's viscosity. All the measured blend values are close to or higher (up to 29.4%) than those of the pure mineral diesel, and the highest values belong to the binary blend of 80 vol% diesel and 20 vol% of FAOCE. In general, ternary blends possess the same or slightly lower viscosity values than binary blends. When the volume fraction of 1-octanol increases in, e.g., 90 vol% ternary blends, from 2.5 to 7.5 vol%, their viscosity slightly decreases, which is contrary to the trend of calculated values based on the additive equation. Although all components are considered non-polar, the presence of 1-octanol (a slightly more polar component) shows an antagonistic influence, resulting in lower viscosity.

3.4.2. Density of Pure Components and Blends

When mutually comparing the pure components' (FAOCE, 1-octanol, and mineral diesel) densities, based on the results presented in Figure 7, FAOCE has the highest density ($881.5 \text{ kg}/\text{m}^3$), mineral diesel the lowest ($826.3 \text{ kg}/\text{m}^3$), whereas the 1-octanol density lies in between ($828.4 \text{ kg}/\text{m}^3$). All the blend density values lie within the limits prescribed by the norm EN 590.

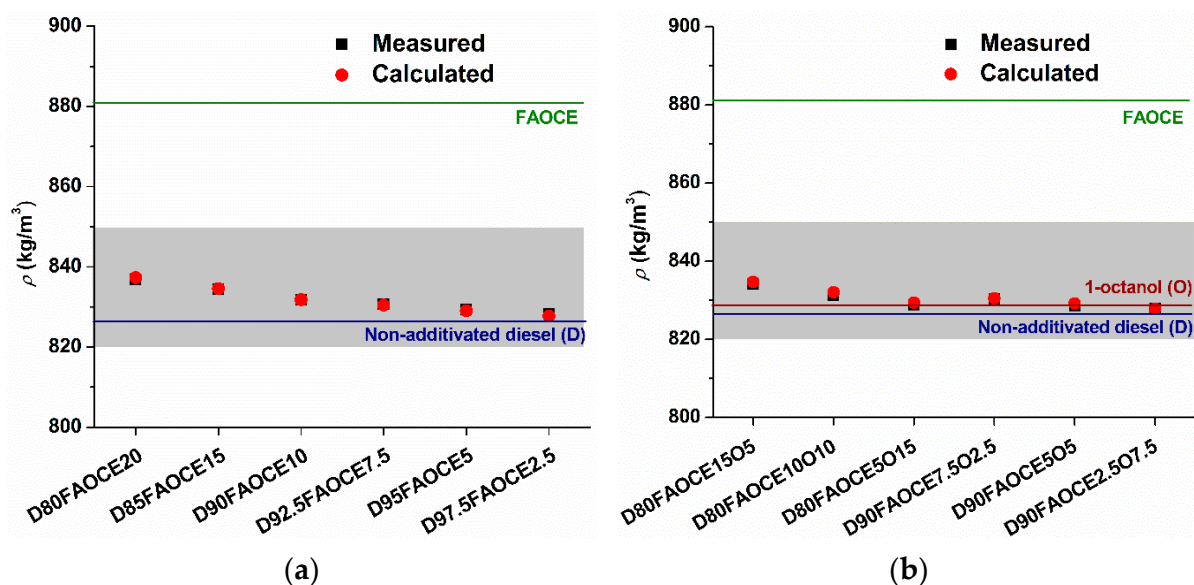


Figure 7. Comparison of measured and calculated density values of binary (a) and ternary (b) blends of 80, 85, 90, 92.5, 95, and 97.5 vol% diesel.

The addition of FAOCE in these binary and ternary blends with mineral diesel and/or 1-octanol resulted in an increase in the blend's density above the pure mineral diesel density value. Again, due to the attractive intermolecular forces between the long chains of FAOCE, diesel, and 1-octanol, as well as good 1-octanol miscibility with other components [24], overall blend density increases with their volume fractions. The welcomed density similarities between 1-octanol and mineral diesel were also reported by Ashok et al. [34] in terms of the improvement of diesel engine combustion and performance characteristics.

3.4.3. Low-Temperature Properties of Pure Components and Blends

The results for the low-temperature properties, obtained via DSC and through conducting the CFPP measurements according to standard EN 116, are given in Figure 8.

1-octanol showed the lowest onset and peak crystallization temperatures, FAOCE the highest, while these values of mineral diesel were in between. Both binary and ternary blends had onset and peak temperature values close to those of mineral diesel, as seen in Figure 8. In the case of binary blends, compared to mineral diesel, crystallization onset and peak values varied between 2.46 °C and 2.16 °C, respectively. On the other hand, with ternary blends, crystallization onset and peak values differed from mineral diesel up to 3.61 °C and 2.45 °C, respectively.

Cold filter plugging point values of mineral diesel, FAOCE, and 1-octanol are -8 , 0 , and -17 °C, respectively. Their binary and ternary blends have CFPP values identical or very close to the mineral diesel. Mutually, there is no visible difference in CFPP values of most of these blends (-7 °C), however, there are some exceptions, i.e., blends D80FAOCE20 and D90FAOCE2.5O7.5 having the CFPP of mineral diesel (-8 °C), as well as D92.5FAOCE7.5 with the CFPP of -6 °C. Nevertheless, all the values are within the repeatability of the methods; therefore, these deviations lack any additional significance. Therefore, the addition of FAOCE up to 20 vol% to the blends do not have a negative effect on the blends' low-temperature properties.

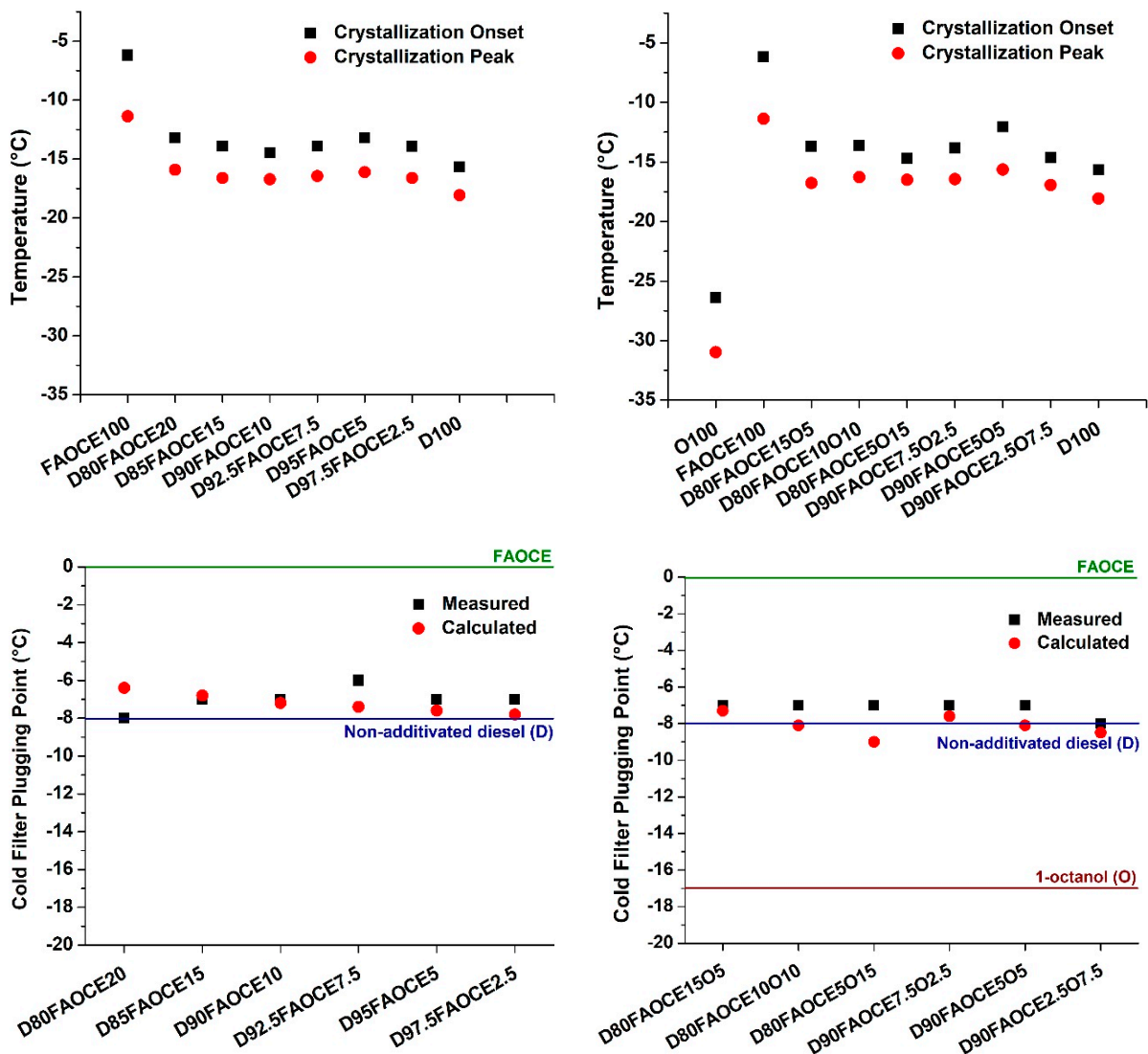


Figure 8. Low-temperature properties (crystallization onset and peak temperatures measured by DSC) and cold filter plugging points of pure components and their binary and ternary blends.

3.4.4. Lubricity and Surface Tension of Pure Components and Blends

Figure 9 represents the results of the lubricity analysis conducted according to the standard EN ISO 12156-1. The results show that the addition of mineral diesel in most cases (except for the blend D80FAOCE20) causes the blend lubricity to decrease, which can be explained by the trend of the values predicted by the additive equation. The addition of 2.5 vol% of FAOCE to the blends reduces the wear scar diameter of mineral diesel to the value that fulfills the standard requirements. Other higher volume fractions of FAOCE further reduce the wear scar diameter, with the minimum value obtained at 15 vol% of FAOCE.

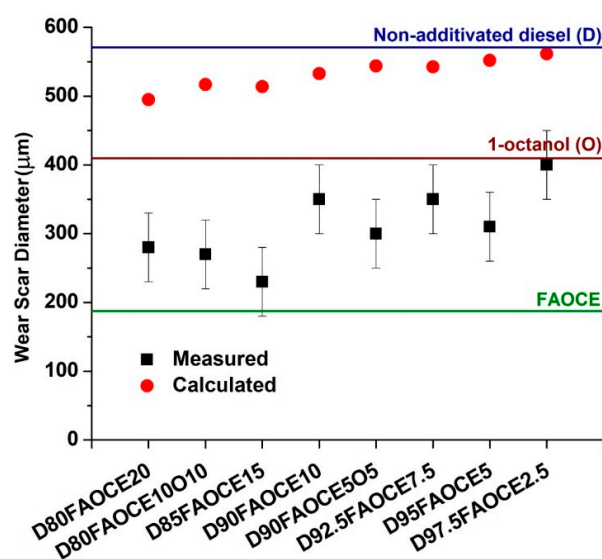


Figure 9. Wear scar diameter values of pure components and their binary and trinary blends with mineral diesel.

If trinary blends of mineral diesel, FAOCE, and 1-octanol (D80FAOCE10O10 and D90FAOCE5O5) are prepared, the lubricity measurements show that the addition of FAOCE and 1-octanol to mineral diesel results in a decrease in the wear scar diameter up to 47.5% from pure mineral diesel. Both of these values fulfill the requirements set by the standard. The increase in FAOCE from 5 to 10 vol% results in a decrease in the wear scar diameter from 300 to 270 μm .

The results for the surface tension measurements are given in Figure 10. FAOCE has the highest surface tension, and mineral diesel has the lowest, while all the blends have these values in between.

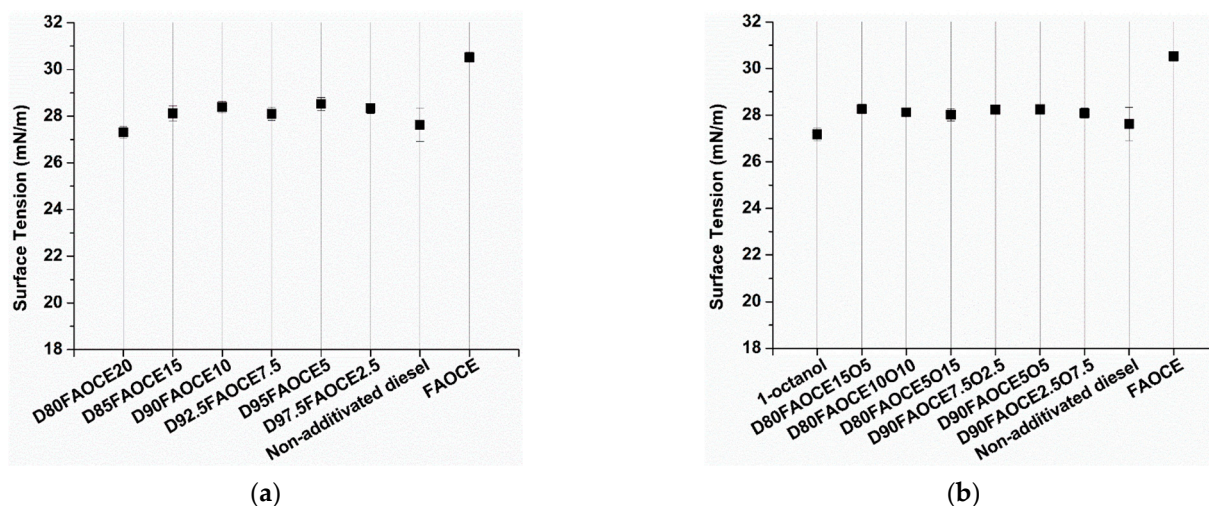


Figure 10. Surface tension values of pure components and their binary (a) and trinary (b) blends with mineral diesel.

4. Conclusions

Fatty acid octyl esters were synthesized by base-catalyzed transesterification reaction using sunflower oil and 1-octanol, and potassium hydroxide as a catalyst. The model obtained by the software Design Expert is significant. The most influential parameters of the transesterification reaction are the molar ratio of the reactants and the mass fraction of the catalyst. Increasing the reaction time and temperature generally increased the reaction

conversion as well, and it is more pronounced when the values of the molar ratio of the reactants and mass fraction of the catalyst were set at low to medium values. At the highest surplus of 1-octanol or the highest amount of catalyst influence of temperature or time of the reaction on the conversion is low to negligible. The obtained optimal results were $T = 40\text{ }^{\circ}\text{C}$, $t = 1\text{ h}$, $A:O = 8.11$ and $w_{\text{cat}} = 2.01$. The numerical optimization predicted the conversion of 100%, while the additional experiment conducted at those conditions gave a conversion of 99%, which is within the 1% accuracy span.

The density of synthesized FAOCE equals 881.5 kg/m^3 , viscosity is equal to $4.613\text{ mm}^2/\text{s}$, wear scar diameter has a value of $190\text{ }\mu\text{m}$, while the CFPP value is $0\text{ }^{\circ}\text{C}$. Measurements showed that FAOCE has a surface tension of 30.52 mN/m .

Mixing of FAOCE with the binary and ternary blends with mineral diesel and 1-octanol results in the fuel whose properties (density, viscosity, lubricity, and CFPP (up to grade C)) comply with the requirements set by the standard EN 590. The differences between densities, viscosities, and CFPP values of non-additivated mineral diesel and obtained blends are minor and are therefore a promising addition to the mineral fuel in terms of similar atomization capabilities. The decrease in FAOCE and the increase in 1-octanol in their blends with mineral diesel generally results in a decrease in blends' densities and viscosities. All blends have a higher surface tension value than non-additivated mineral diesel. Lubricity is improved by the addition of FAOCE and 1-octanol to non-additivated mineral diesel.

To sum up, since 1-octanol can be blended into diesel at higher concentrations without affecting engine performance, this eliminates the need to remove 1-octanol from biodiesel during the purification step, making the process less complex and more economical. Other application properties such as density, viscosity, and surface tension are within the required limits, which means that the blends will have similar fuel atomization in compression ignition engines.

Supplementary Materials: The following supporting information can be downloaded at: <https://www.mdpi.com/article/10.3390/en16073071/s1>. Figure S1: Conversion determination via nuclear magnetic resonance—integration of the areas under the signals at around 2.3 and 4.0 ppm; Figure S2: Comparison of calculated and experimentally determined conversion values; Figure S3: Graphical representation of the distribution of residues, r_s depending on the ordinal number of the experiment; Figure S4: The 3D plots obtained when the molar ratio of the reactants was the lowest (4:1) and the value of the mass fraction of the catalyst was the lowest (1%, left), medium (2%, in the middle) and the highest (3%, right); Figure S5: The 3D plots obtained when the molar ratio of the reactants was medium (7:1) and the value of the mass fraction of the catalyst was the lowest (1%, left), medium (2%, in the middle) and the highest (3%, right); Figure S6: The 3D plots obtained when the molar ratio of the reactants was the highest (10:1) and the value of the mass fraction of the catalyst was the lowest (1%, left), medium (2%, in the middle) and the highest (3%, right); Figure S7. An example of the differential scanning calorimetry curve analysis; Table S1: Part of ANOVA for quadratic model; Table S2: Composition of the prepared blends (D—mineral diesel without additives, FAOCE—fatty acid octyl esters, O—1-octanol); Table S3: The property results of diesel, 1-octanol, FAOCE and their blends.

Author Contributions: Conceptualization, F.F.; methodology, M.R.; formal analysis, M.G. and M.R.; investigation, L.K., J.P.V., M.G. and M.R.; resources, F.F.; data curation, F.F. and M.R.; writing—original draft preparation, M.G.; writing—review and editing, F.F. and M.R.; visualization, M.G.; supervision, F.F.; project administration, F.F.; funding acquisition, F.F. All authors have read and agreed to the published version of the manuscript.

Funding: This research was conducted within the Project of the Croatian Science Foundation Development of functional biofuels and (bio)additives and characterization of blends with mineral fuels (FunBioFA, UIP-2019-04-5242).

Data Availability Statement: The data presented in this study are available on request from the corresponding author.

Conflicts of Interest: The authors declare no conflict of interest. The funders had no role in the design of the study; in the collection, analyses, or interpretation of data; in the writing of the manuscript; or in the decision to publish the results.

References

1. Suresh, M.; Jawahar, C.P.; Richard, A. A review on biodiesel production, combustion, performance, and emission characteristics of non-edible oils in variable compression ratio diesel engine using biodiesel and its blends. *Renew. Sustain. Energy Rev.* **2018**, *92*, 38–49. [[CrossRef](#)]
2. Silitonga, A.S.; Masjuki, H.H.; Mahlia, T.M.I.; Ong, H.C.; Chong, W.T.; Boosroh, M.H. Overview properties of biodiesel diesel blends from edible and non-edible feedstock. *Renew. Sustain. Energy Rev.* **2010**, *22*, 346–360. [[CrossRef](#)]
3. Xue, J.; Grift, T.E.; Hansen, A.C. Effect of biodiesel on engine performances and emissions. *Renew. Sustain. Energy Rev.* **2011**, *15*, 1098–1116. [[CrossRef](#)]
4. Atabania, A.E.; Silitonga, A.S.; Badruddina, I.A.; Mahlia, T.M.I.; Masjukia, H.H.; Mekhilefd, S. A comprehensive review on biodiesel as an alternative energy resource and its characteristics. *Renew. Sustain. Energy Rev.* **2012**, *16*, 2070–2093. [[CrossRef](#)]
5. Li, L.; Jianxin, W.; Zhi, W.; Jianhua, X. Combustion and emission characteristics of diesel engine fueled with diesel/biodiesel/pentanol fuel blends. *Fuel* **2015**, *156*, 211–218. [[CrossRef](#)]
6. Biswas, S.; Katiyar, R.; Gurjar, B.R.; Pruthi, V. Biofuels and Their Production Through Different Catalytic Routes. *Chem. Biochem. Eng. Q.* **2017**, *31*, 47–62. [[CrossRef](#)]
7. Salvi, B.L.; Subramanian, K.A.; Panwar, N.L. Alternative fuels for transportation vehicles: A technical review. *Renew. Sustain. Energy Rev.* **2013**, *25*, 404–419. [[CrossRef](#)]
8. Mofijur, M.; Rasul, M.G.; Hyde, J.; Azad, A.K.; Mamat, R.; Bhuiya, M.M.K. Role of biofuel and their binary (diesel-biodiesel) and ternary (ethanol-biodiesel-diesel) blends on internal combustion engines emission reduction. *Renew. Sustain. Energy Rev.* **2016**, *53*, 265–278. [[CrossRef](#)]
9. Kumar, S.; Cho, J.H.; Park, J.; Moon, I. Advances in diesel–alcohol blends and their effects on the performance and emissions of diesel engines. *Renew. Sustain. Energy Rev.* **2013**, *22*, 46–72. [[CrossRef](#)]
10. Gotovuša, M.; Medić, M.; Faraguna, F.; Šibalić, M.; Konjević, L.; Parlov Vuković, J.; Racar, M. Fatty acids propyl esters: Synthesis optimization and application properties of their blends with diesel and 1-propanol. *Renew. Energy* **2022**, *185*, 655–664. [[CrossRef](#)]
11. Wang, P.S.; Tat, M.E.; Gerpen, J.V. The Production of Fatty Acid Isopropyl Esters and Their Use as a Diesel Engine Fuel. *J. Am. Oil. Chem. Soc.* **2005**, *82*, 845–849. [[CrossRef](#)]
12. Sendzikiene, E.; Sinkuniene, D.; Kazanceva, I.; Kazancev, K. Optimization of low quality rapeseed oil transesterification with butanol by applying the response surface methodology. *Renew. Energy* **2016**, *87*, 266–272. [[CrossRef](#)]
13. Konovalov, S.; Patrylak, L.; Zubenko, S.; Okhrimenko, M.; Yakovenko, A.; Levterov, A.; Avramenko, A. Alkali synthesis of fatty acid butyl and ethyl esters and comparative bench motor testing of blended fuels on their basis. *Chem. Chem. Technol.* **2021**, *15*, 105–117. [[CrossRef](#)]
14. Hanh, H.D.; Dong, N.T.; Okitsu, K.; Nishimura, R.; Maeda, Y. Biodiesel production through transesterification of triolein with various alcohols in an ultrasonic field. *Renew. Energy* **2009**, *34*, 766–768. [[CrossRef](#)]
15. Liang, X.; Wu, F.; Xie, Q.; Wu, Z.; Cai, J.; Zheng, C.; Fu, J.; Nie, Y. Insights into biobased epoxidized fatty acid isobutyl esters from biodiesel: Preparation and application as plasticizer. *Chin. J. Chem. Eng.* **2021**, *44*, 41–50. [[CrossRef](#)]
16. Malins, K.; Kampars, V.; Kampare, R.; Prilucka, J.; Brinks, J.; Murnieks, R.; Apseniece, L. Properties of rapeseed oil fatty acid alkyl esters derived from different alcohols. *Fuel* **2014**, *137*, 28–35. [[CrossRef](#)]
17. de Oliveira, V.F.; Parente, E.J.S., Jr.; Manrique-Rueda, E.D.; Cavalcante, C.L., Jr.; Luna, F.M.T. Fatty acid alkyl esters obtained from babassu oil using C1–C8 alcohols and process integration into a typical biodiesel plant. *Chem. Eng. Res. Des.* **2020**, *160*, 224–232. [[CrossRef](#)]
18. Faraguna, F.; Racar, M.; Glasovac, Z.; Jukić, A. Correlation Method for Conversion Determination of Biodiesel Obtained from Different Alcohols by ¹H NMR Spectroscopy. *Energy Fuels* **2017**, *31*, 3943–3948. [[CrossRef](#)]
19. Rajesh; Kumar, B.; Saravanan, S. Use of higher alcohol biofuels in diesel engines: A review. *Renew. Sustain. Energy Rev.* **2016**, *60*, 84–115. [[CrossRef](#)]
20. Bharti, A.; Banerjee, T. Reactive force field simulation studies on the combustion behavior of n-octanol. *Fuel Process. Technol.* **2016**, *152*, 132–139. [[CrossRef](#)]
21. Imdadul, H.K.; Masjuki, H.H.; Kalam, M.A.; Zulkifli, N.W.M.; Alabdulkarem, A.; Rashed, M.M.; Teoh, Y.H.; Howa, H.G. Higher alcohol–biodiesel–diesel blends: An approach for improving the performance, emission, and combustion of a light-duty diesel engine. *Energy Convers. Manag.* **2016**, *111*, 174–185. [[CrossRef](#)]
22. Zhang, Z.H.; Chua, S.M.; Balasubramanian, R. Comparative evaluation of the effect of butanol–diesel and pentanol–diesel blends on carbonaceous particulate composition and particle number emissions from a diesel engine. *Fuel* **2016**, *176*, 40–47. [[CrossRef](#)]
23. Yilmaz, N.; Atmanli, A.; Trujillo, M. Influence of 1-pentanol additive on the performance of a diesel engine fueled with waste oil methyl ester and diesel fuel. *Fuel* **2017**, *207*, 461–469. [[CrossRef](#)]
24. Atabani, A.E.; Kulthoom, S.A. Spectral, thermoanalytical characterizations, properties, engine and emission performance of complementary biodiesel-diesel-pentanol / octanol blends. *Fuel* **2020**, *282*, 118849. [[CrossRef](#)]

25. Atmanli, A. Comparative analyses of diesel–waste oil biodiesel and propanol, *n*-butanol or 1-pentanol blends in a diesel engine. *Fuel* **2016**, *176*, 209–215. [[CrossRef](#)]
26. Falbe, J.; Bahrmann, H.; Lipps, W.; Mayer, D.; Frey, G.D. *Alcohols, Aliphatic*. *Ullmann's Encyclopedia of Industrial Chemistry*, 6th ed.; Wiley-VCH Verlag GmbH & Co., KGaA: Weinheim, Germany, 2013; p. 14.
27. Dellomonaco, C.; Clomburg, J.M.; Miller, E.N.; Gonzalez, R. Engineered reversal of the β -oxidation cycle for the synthesis of fuels and chemicals. *Nature* **2011**, *476*, 355–359. [[CrossRef](#)] [[PubMed](#)]
28. Machado, H.B.; Dekishima, Y.; Luo, H.; Lan, E.L.; Liao, J.C. A selection platform for carbon chain elongation using the CoA-dependent pathway to produce linear higher alcohols. *Metab. Eng.* **2012**, *14*, 504–511. [[CrossRef](#)]
29. Marcheschi, R.J.; Li, H.; Zhang, K.; Noey, E.L.; Kim, S.; Chaubey, A.; Houk, K.N.; Liao, J.C. A Synthetic Recursive “+1” Pathway for Carbon Chain Elongation. *ACS Chem. Biol.* **2012**, *7*, 689–697. [[CrossRef](#)]
30. Sattayawat, P.; Yunus, I.S.; Jones, P.R. Bioderivatization as a concept for renewable production of chemicals that are toxic or poorly soluble in the liquid phase. *Proc. Natl. Acad. Sci. USA* **2020**, *117*, 1404–1413. [[CrossRef](#)]
31. Akhtar, M.K.; Dandapani, H.; Thiel, K.; Jones, P.R. Microbial production of 1-octanol: A naturally excreted biofuel with diesel-like properties. *Metab. Eng. Commun.* **2015**, *2*, 1–5. [[CrossRef](#)]
32. Mehner, C.R.; Incha, M.R.; Politz, M.C.; Pflieger, B.F. Anaerobic Production of Medium-Chain Fatty Alcohols via a β -Reduction Pathway. *Metab. Eng.* **2018**, *48*, 63–71. [[CrossRef](#)] [[PubMed](#)]
33. Lozada, N.J.H.; Simmons, T.R.; Xu, K.; Jindra, M.A.; Pflieger, B.F. Production of 1-octanol in *Escherichia coli* by a high flux thioesterase route. *Metab. Eng.* **2020**, *61*, 352–359. [[CrossRef](#)] [[PubMed](#)]
34. Ashok, B.; Nanthagopal, K.; Anand, V.; Aravind, K.M.; Jeevanantham, A.K.; Balusamy, S. Effects of *n*-octanol as a fuel blend with biodiesel on diesel engine characteristics. *Fuel* **2019**, *235*, 363–373. [[CrossRef](#)]
35. Sreeprasanth, P.S.; Srivastava, R.; Srinivas, D.; Ratnasamy, P. Hydrophobic, solid acid catalysts for production of biofuels and lubricants. *Appl. Catal. Gen.* **2006**, *314*, 148–159. [[CrossRef](#)]
36. Putra, T.W.; Hardiansyah, R.; Lubis, M.R.; Supardan, M.D. Intensification of biolubricant synthesis from waste cooking oil using tetrahydrofuran as co-solvent. *IOP Conf. Ser. Mater. Sci.* **2020**, *845*, 012009. [[CrossRef](#)]
37. Chowdhury, A.; Sarkar, D.; Mitra, D. Esterification of Free Fatty Acids Derived from Waste Cooking Oil with Octanol: Process Optimization and Kinetic Modeling. *Chem. Eng. Technol.* **2016**, *39*, 730–740. [[CrossRef](#)]
38. Chowdhury, A.; Chakraborty, R.; Mitra, D.; Biswas, D. Optimization of the production parameters of octyl ester biolubricant using Taguchi's design method and physico-chemical characterization of the product. *Ind. Crop. Prod.* **2014**, *52*, 783–789. [[CrossRef](#)]
39. Cai, Z.; Wu, S.; Sun, G.; Niu, Y.; Zheng, D.; Peng, S.; Yang, W.; Wang, Y.; Yang, D. High-Purity Fatty Acid *n*-Octyl Esters from Housefly (*Musca domestica* L.) Larval Lipids, a Potential New Biolubricant Source. *Energy Fuels* **2017**, *31*, 10966–10974. [[CrossRef](#)]
40. Porwal, J.; Karanwal, N.; Kaul, S.; Jain, S.L. Carbocatalysis: N-doped reduced graphene oxide catalyzed esterification of fatty acids with long chain alcohols. *N. J. Chem.* **2016**, *40*, 1547–1553. [[CrossRef](#)]
41. Bassi, J.J.; Todero, L.M.; Lage, F.A.P.; Khedy, G.I.; Ducas, J.D.; Custódio, A.P.; Pinto, M.A.; Mendes, A.A. Interfacial activation of lipases on hydrophobic support and application in the synthesis of a lubricant ester. *Int. J. Biol. Macromol.* **2016**, *92*, 900–909. [[CrossRef](#)]
42. Laudani, C.G.; Habulin, M.; Primožic, M.; Knez, Z.; Della Porta, G.; Reverchon, E. Optimisation of *n*-octyl oleate enzymatic synthesis over Rhizomucor miehei lipase. *Bioproc. Biosyst. Eng.* **2006**, *29*, 119–127. [[CrossRef](#)] [[PubMed](#)]
43. Habulin, M.; Krmelj, V.; Knez, Ž. Synthesis of Oleic Acid Esters Catalyzed by Immobilized Lipase. *J. Agric. Food. Chem.* **1996**, *44*, 338–342. [[CrossRef](#)]
44. Barange, S.H.; Raut, S.U.; Bhansali, K.J.; Balinge, K.R.; Patle, D.S.; Bhagat, P.R. Biodiesel production via esterification of oleic acid catalyzed by Brønsted acid-functionalized porphyrin grafted with benzimidazolium-based ionic liquid as an efficient photocatalyst. *Biomass Convers. Biorefinery* **2021**, *13*, 1873–1888. [[CrossRef](#)]
45. Khajone, V.B.; Bhagat, P.R. Brønsted acid functionalized phthalocyanine on perylene diimide framework knotted with ionic liquid: An efficient photo-catalyst for production of biofuel component octyl levulinate at ambient conditions under visible light irradiation. *Fuel* **2020**, *279*, 118390. [[CrossRef](#)]
46. Sidharth; Kumar, N. Comparison of properties of ternary fuel blends of diesel-octanol with biodiesel. *IOP Conf. Ser. Mater. Sci. Eng.* **2019**, *691*, 012050. [[CrossRef](#)]
47. Pratas, M.J.; Freitas, S.V.D.; Oliveira, M.B.; Monteiro, S.C.; Lima, A.S.; Coutinho, J.A.P. Biodiesel Density: Experimental Measurements and Prediction Models. *Energy Fuels* **2011**, *25*, 2333–2340. [[CrossRef](#)]
48. Verduzco, L.F.R. Density and viscosity of biodiesel as a function of temperature: Empirical models. *Renew. Sustain. Energy Rev.* **2013**, *19*, 652–665. [[CrossRef](#)]
49. Parente, R.C.; Nogueira, C.A.; Carmo, F.R.; Lima, L.P.; Fernandes, F.A.N.; Santiago-Aguiar, R.S.; de Sant'Ana, H.B. Excess Volumes and Deviations of Viscosities of Binary Blends of Sunflower Biodiesel + Diesel and Fish Oil Biodiesel + Diesel at Various Temperatures. *J. Chem. Eng. Data.* **2011**, *56*, 3061–3067. [[CrossRef](#)]
50. Peterson, C.L.; Auid, D.L. Proceedings of Solid Fuel Conversion for the Transportation Sector. *ASME* **1991**, *12*, 45–54.
51. Knothe, G.; Steidley, K.R. Kinematic viscosity of biodiesel fuel components and related compounds. Influence of compound structure and comparison to petrodiesel fuel components. *Fuel* **2005**, *84*, 1059–1065. [[CrossRef](#)]
52. Fazal, M.A.; Haseeb, A.S.M.A.; Masjuki, H.H. Investigation of friction and wear characteristics of palm biodiesel. *Energy Convers. Manag.* **2013**, *67*, 251–256. [[CrossRef](#)]

53. Kumar, N.; Varun; Chauhan, S. Analysis of tribological performance of biodiesel. *Proc. Inst. Mech. Eng.* **2014**, *228*, 797–807. [[CrossRef](#)]
54. Sulek, M.W.; Kulczycki, A.; Malysa, A. Assessment of lubricity of compositions of fuel oil with biocomponents derived from rape-seed. *Wear* **2010**, *268*, 104–108. [[CrossRef](#)]
55. Tang, H.; Salley, S.O.; Ng, K.Y.S. Fuel properties and precipitate formation at low temperature in soy-, cottonseed-, and poultry fat-based biodiesel blends. *Fuel* **2008**, *87*, 3006–3017. [[CrossRef](#)]
56. Park, J.Y.; Kim, D.K.; Lee, J.P.; Park, S.C.; Kim, Y.J.; Lee, J.S. Blending effects of biodiesels on oxidation stability and low temperature flow properties. *Bioresour. Technol.* **2008**, *99*, 1196–1203. [[CrossRef](#)]
57. Kim, J.K.; Yim, E.S.; Jeon, C.H.; Jung, C.S.; Han, B.H. Cold Performance of Various Biodiesel Fuel Blends at Low Temperature. *Int. J. Automot. Technol.* **2012**, *13*, 293–300. [[CrossRef](#)]
58. Myers, R.H.; Montgomery, D.C. *Response Surface Methodology, Process and Product Optimization Using Designed Experiments*, 2nd ed.; John Wiley & Sons, Inc.: New York, NY, USA, 2002; pp. 46–62.

Disclaimer/Publisher’s Note: The statements, opinions and data contained in all publications are solely those of the individual author(s) and contributor(s) and not of MDPI and/or the editor(s). MDPI and/or the editor(s) disclaim responsibility for any injury to people or property resulting from any ideas, methods, instructions or products referred to in the content.